The Markov behavior in PERC solar cells based on transient photovoltage process

YIFENG HE[1,2,3,*], DAVID PEREZ DE LARA[1], XINGZHU WANG[1], YONGGANG GAO[1], DELIN JIN[1], HAIQUAN ZHOU[1], BINGJIE ZHU[4], HUAYU FENG[5,6]
[1]*Zhejiang Beyondsun Green Energy Technology CO., LTD., Huzhou, Zhejiang, 313200, China*
[2]*Zhejiang Beyondsun PV CO., LTD., Huzhou, Zhejiang, 313200, China*
[3]*Zhejiang Beyondsun New Energy Development CO., LTD., Huzhou, Zhejiang, 313200, China*
[4]*Wuxi Institution of Supervision & Testing on Product Quality, Wuxi, Jiangsu, 214101, China*
[5]*CETC Deqing Huaying Electronics CO., LTD., Huzhou, Zhejiang, 313200, China*
[6]*College of Materials, Shandong University, Jinan, 250014, China*

The Passivated Emitter and Rear Cell (PERC) structures were widely applied in the p-Type silicon solar cell with the advancement of technology. However, the behaviors of carriers in PECRC bulks were difficult to be predicted due to the Brownian movement and scattering. Here, we have simulated the charge behaviors of PERC based on the Markov Chain in a transient and open circuit (OC) condition. In OC condition, charge carriers were jumped among various states without exporting to external circuit. Hence, the Markov Chain can be used to predict the probability of carriers in various states and then give an expectation of voltage dynamic. In the experimental result, it can be seen that the tendency of voltage was well fixed with the simulation under thermal equilibrium (T=300 K) condition. Once the equilibrium was broken by the thermal injection, the increasement of deep-level traps will accelerate the recombination rate. This work can also be applied in other field such as photo detectors and light emitting diodes (LEDs) to predict the charge behaviors.

(Received May 5, 2022; accepted February 6, 2023)

Keywords: PERC solar cells, Transient photovoltage, Open circuit recombination, Markov chain

1. Introduction

Solar cells have occupied an important place in renewable energy market due to its low cost, stability and high efficiency in energy conversion [1-3]. Though the new materials such as organic [4] and perovskite [5] are emerging in the scientific community, silicon is still championed the commercial market [6]. To further dig the potentials of silicon solar cells, various solar cell structures have been proposed, such as Tunnel Oxide Passivated Contact (Top-Con) [7] and Heterojunction technology (HJT) [8], which consolidate the solar cell' share in renewable energy market. The basic function of any type of solar cells is to convert energy from photons to electric carriers. Hence, understanding the behaviors of charge carriers is an important topic for solar cells. The dynamic of electrons or holes are complicated inside of solar cells but approximately summarized into four steps: (1) the photon absorption and electron excitation [9], electrons will be excited from ground states to excited states and leave holes in original positions; (2) the charge transportation [10], the electron-hole charge carriers separated and transfer to each charge transportation layer; (3) the charge extraction [11], carriers are drifted to electrodes and then extracted to external circuit; (4) an important and ambiguous step, the charge recombination [12], carriers are recombined by opposite charge states or impurity traps. In summary, the dynamic of charge carriers was mixed with previously mentioned four steps simultaneously which is difficult to predict or distinguish the behavior of charge carriers. Meanwhile, understanding the behaviors of charge carriers are helpful in the further promotion of the solar cell performance in energy conversion. Hence, the scientific community has spent decades in explaining the charge behaviors based on semiconductor physics in solar cell [13-15]. However, it is difficult to describe charge behavior due to the uncertainty effect and Brownian movement. Hence, an appropriate statistical methodology is essential to present the behaviors inside of solar cells, and the digging of charge behaviors is beneficial to further enhance the power conversion efficiency (PCE) of solar cells. Among all types of silicon cells, the Passivated Emitter and Rear Cell (PERC) [16-18] has dramatically decreased the surface recombination due to the passivation methodology which has provided a distinguishable sample for the investigation of bulk recombination. In this article, we have used Markov Chain to investigate the charge behaviors in Open Circuit (OC) condition for PERC solar cells. The results of simulate demonstrated the Markov Chain obtain the ability

to predict the probability of carriers in various states and the give an expectation of voltage dynamic. In the experimental result, it can be seen that the tendency of voltage was well fixed with the simulation under thermal equilibrium (T = 300 K) condition. However, once the equilibrium was broken by the thermal injection, the increasement of deep-level traps will accelerate the recombination rate. The investigation of carrier behavior can also be applied in other optoelectronic applications such as photo detectors and light emitting diodes (LEDs).

2. The Markov approach

The development of passivation and emitter technology [16-18] in PERC have dramatically decreased the surface recombination, which means the generation of photo induced charge occurs without the process of surface recombination. As previously described in the introduction part. The step (1) of photocurrent generation only occurs under light irradiation, as we have assumed here the injection signal was a pulse function. In another word, step (2) and step (4) directly relate to the photon injection and trap densities. For a specific charge carrier (electron or hole), it was difficult to explain the its behaviors due to the combination of electrical drift [19] and thermal diffusion [20]. However, in OC condition, the non-geminate recombination and carrier extraction (step 3) is negligible [21]. Hence, those physical processes can be summarized into 3 states with transfer chains (Schematic in Fig. 1).

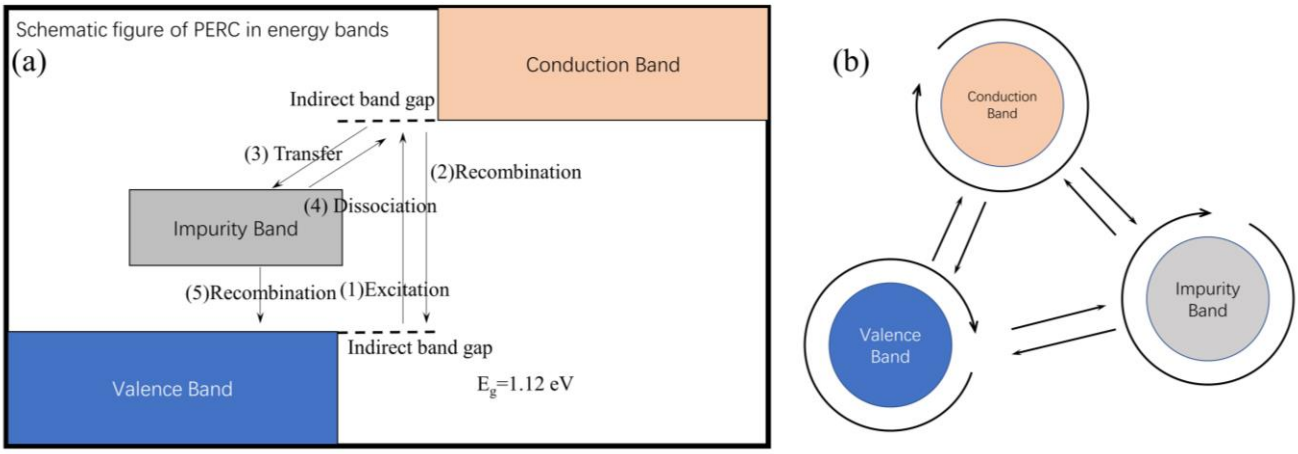

Fig. 1. (a) The schematic figure of charge dynamic process of carriers in the conduction band, valence and impurity band in PERCs, (b) the simplified diagram of the carrier dynamic process (color online)

As Fig. 1 (a) described, charge carrier only jumped among 3 states in OC condition, and it will undergo mutual transport, recombination and transition in conduction band without extracting to external circuit. The more concise description of the carrier jump process was shown in Fig. 1 (b). It can be seen that all charge carriers were moved conditionally on the present states of PERCs which followed the description of Markov Properties [22]. The charge behaviors satisfy the Markov Property indicated that predications for future of the process based solely on their present states regardless with previous behaviors. Hence, the dynamic of charges can be written into a Markov Chain as shown in Eq. (1):

$$P = \begin{pmatrix} P_{g\to g} & P_{g\to e} & P_{g\to r} \\ P_{e\to g} & P_{e\to e} & P_{e\to r} \\ P_{r\to g} & P_{r\to e} & P_{r\to r} \end{pmatrix} \quad (1)$$

where the P is the probability of Markov Jump on a specified time, g represents ground state on valence band, e represents the excited state on conduction band, r represents recombination state on impurity band.

It was worthy to mention that the Markov described the physical model in OC condition. Hence, all charges were finally fall into ground state due to the thermal equilibrium at 300 K. In Eq. (1) the row of matrix means the was the origin of charge carriers at present time point and the column meant the direction of charge carriers. The $P_{i\to j}$ represented the probability that charge carrier jump from state i to state j on statistics with probability of $dn_{i\to j}/dn$. Note, the sum of each column should equal to 1 means all carriers were limited in the PERC bulks (Prohibition of charge extraction). Also, the statistical number of carriers can be approximately calculated by the size of silicon bulk and the volume of p-n junction [23] up limitation to 2×10^{23} cm^{-3}. In the experimental section, the doping density of silicon gave a carrier density to only 1×10^{18} cm^{-3}.

Then the jump process was divided into 2 parts according to the pulse function of laser injection. The laser was injecting photons in the 1st part where charge carriers were started to be excited to conduction band and free

carriers were falling down to ground state or trapped by impurities. Hence the carriers were moving among from or to various states as described in Eq. (1). Once the light irradiation was turned off, the jump process then came to the 2^{ed} part, electrons were banned from ground state to excited state. Meanwhile, excited carriers started to fall down due to the limitation of life time. Then the probability of each states was tuned to another condition which was determined by the quantities of carriers in each state.

3. Experimental

The PERC Cells were provided by Wuxi Sunteck-power Co. Ltd, and dual characterized by a national photovoltaic center (CPVT) to ensure the performance of solar cells. In details, the mono-crystal substrates were fabricated into solar cells with the standard PERC processing which sequenced from texture & clean to metallization. The wafer specification was resistivity 1–3 Ω·cm, thickness up to 190 μm with size of 156 mm × 156 mm. Before the deposition of passivation layers, all substrates were saw-damage etched and second time of surface texturing to reduce the interfacial traps by HNO_3/HF solution, and followed with an HCl/HF cleaning. Then a laser (532 nm, CW, 10 W) doping technique were applied to form the emitter with sheet resistance around 90 Ω/sq. The he AlO:H_x layer was deposited using standard Roth & Rau® remote microwave plasma enhanced chemical vapor deposition (PECVD) systems, meanwhile, the SiN_x:H layer were deposited through Centrotherm® PECVD systems. After the printing of electrodes, the solar cells were characterized by a Keithley® 2450 source unit for the *I-V* performance under the irradiation of standard AM 1.5G condition (1000 W/m^2).

To explain the carrier behavior in OC condition, we designed an experiment named as transient-photovoltage (TPV) to check the carrier behaviors in isolated semiconductor bulk (Schematic figure were shown in Fig. 2). The TPV were performed by home-made systems based on PERC solar cells. The setup of TPV was consisted with a 532 nm pulsed laser (OSRAM® 10 mW, 125 Hz), a power resistor (10 MΩ, $\Delta R \leq \pm 00.1\%$), a constant white light source (OSRAM® 10W, full spectrum) and a high-resolution oscilloscope (PicoScope® 2242B). In the OC condition, the device was perturbed by 532 nm pulsed laser after the device was stabilized under white light, and the oscilloscope will record the new carriers' generation and the recombination process.

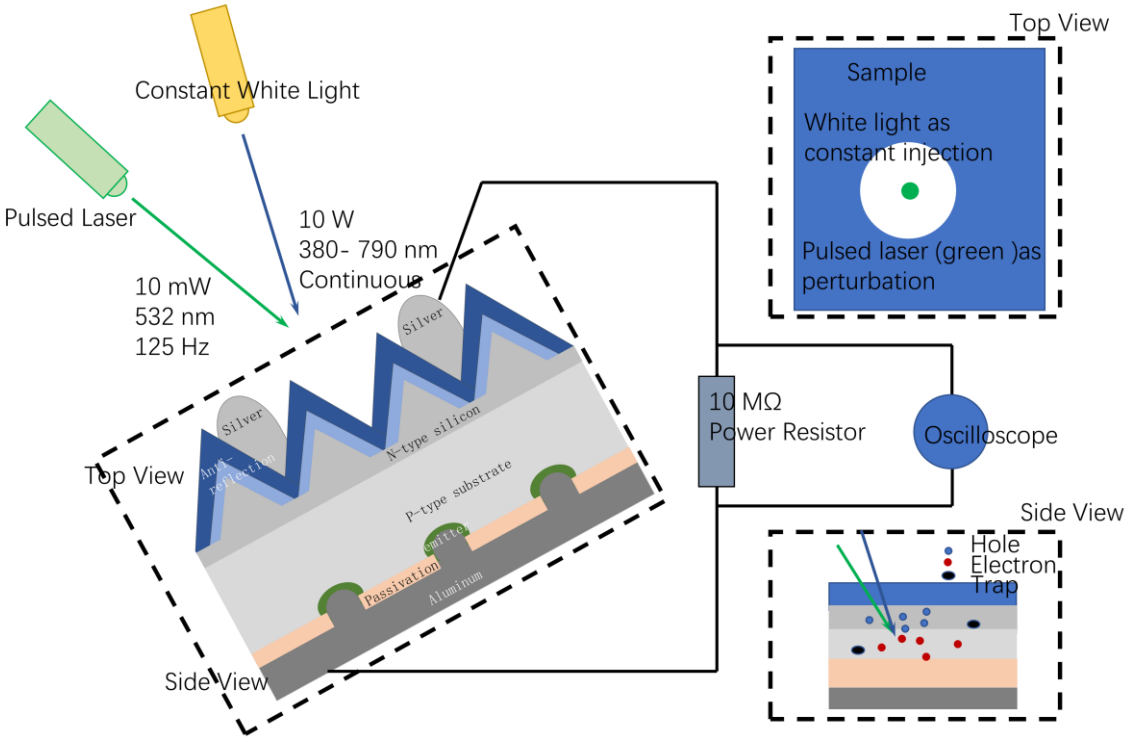

Fig. 2. The schematic figure of TPV setups (color online)

4. Result and discussion

The PCE were initially characterized and shown in Fig. 3 to confirm the performance of tested sample.

It can be seen that the PERC was performed perfectly with the technique of surface passivation, the Fill Factor extended over 80% and current density also reach over 40 mA/cm^2. The PCE has arrived 22.85% indicating that the PERC was working on an ideal condition without effects of heavy density of traps.

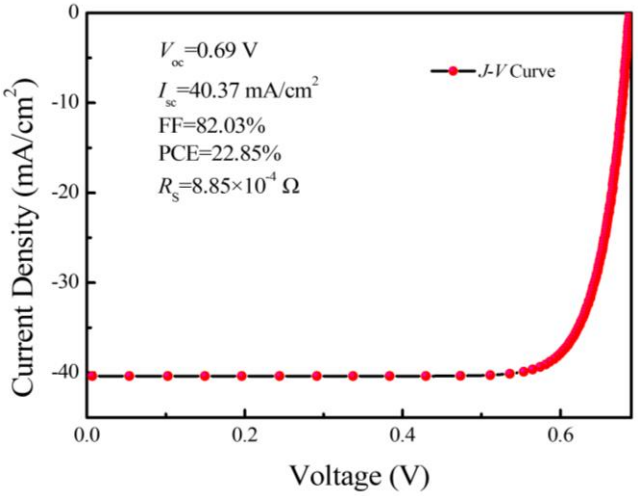

Fig. 3. The Current Density (J)-Voltage (V) curve of tested PERC sample (color online)

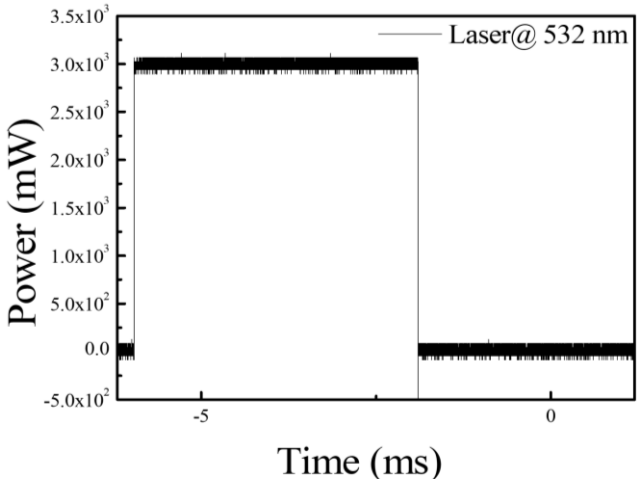

Fig. 4. The average power of laser output

The laser was designed by home built integrated circuit with triggered edge in nanosecond range to ensure the light injection could generate a pulse input signal. The laser power was traced by a powermeter and shown in Fig. 4. Tough the power output fluctuated in microwatt range but the noise can be influenced by both laser and powermeter. Meanwhile, the laser raising edge and falling edge changed sharply which provided an ideal pulse light signal. Hence, we can approximately establish a stable injection signal for the following characterization. Meanwhile, the injection laser power can be calculated as number of stable photons per second at 532 nm of

$$n_{\text{pho}}=Pct/(h\lambda t) \tag{2}$$

where the n_{pho} is the number of photons per second, P is the laser power, t is time, h is plank constant and λ is wavelength of laser.

It can be counted that the photon population can be up to 2.535×10^{46}/s. Meanwhile, the spot size of laser was 2 cm^2. Hence the photon population density was around 1.268×10^{46}/(cm^3·s) which was still 28 magnitudes higher than that of carriers on ground states. It indicated that most charge carriers can be excited to higher states under the laser irradiation. Traps states were characterized by microwave photoconductivity decay within 30 μm thickness of PERC to a lifetime of 600 μs which is very close to the reference result [24]. Shao has predicted that the traps was approximately 1 ppma in pn junctions which means the trap density was around 1×10^{12} cm^{-3}.

Hence, once the pulse laser irradiates on the device, the PERC will arrive stable state after certain lifetime due to the RC (resistance and capacitance) differential property. Meanwhile, abundant carriers were rapidly jumped among various states in the cell. The behaviors of carriers are worthy discussed that how to form a charging and discharging process in micro-nano range and ultrafast time scope. As previous introduction in Eq. (1), the movement of carriers, which can be referred to as continuous time signals, were converted to discrete time signals. In statistical analysis, this movement was also defined as the probability of appearing between various states. For the next jump point, the probability can be following conducted to P^2 and the final probability of carrier movement was P^n, where the n is the discrete time of the whole physical process. Then the final probability can be written as

$$\mathrm{E}\begin{bmatrix} g \\ e \\ i \end{bmatrix} = P^n \begin{matrix} g \\ (e) \\ i \end{matrix} \tag{3}$$

where E is the expectation, P is the Markov jump probability, and g, e and i were states as previously introduced in Eq. (1). According to the law of the Markov Chain, the Markov Jump probability of the carrier can be expressed as

$$P^n = \sqrt{\frac{2}{\pi t}} \int_x^{\infty} e^{-\frac{u^2}{2t}} du, \quad 0 < t < T_x \tag{4}$$

$$P^n = 1, \qquad T_x < t < T_x + T_1 \tag{5}$$

$$P^n = \frac{1}{\sqrt{2\pi t}} \int_{-\infty}^{x} e^{-\frac{u^2}{2t}} du, \; T_x + T_1 < t \tag{6}$$

where the t is the carrier movement time, T_1 is the laser pulse width, T_x is the time of carrier transition from valence band to conduction band or impurity band in a random process, x is the state of the existence of carriers in OC condition. The internal voltage distribution can be easily written as

$$V_{out}(t)=V_{input}(t)*\delta(t)+RC\mathrm{d}V_{out}(t)/\mathrm{d}t \quad (7)$$

where the V_{out} is the voltage between the electrodes of PERC, in OC condition, the sandwich structure become a capacitor rather than a solar cell, the * is a convolutions operation. R is the series resistance of sample and C is the static capacitance of PERC. Therefore, we can further determine that the voltage value during the period with Markov process is

$$V(t) = V_{out}(t) \cdot P^n \quad (8)$$

We simulated the dynamics of the internal carriers with Markov Jumps according to Eq. 8. The results of simulation and the TPV experiments were shown in Fig. 5. The experimental result exhibited a slow charging and discharging effect with lifetime of 175 μs and 782 μs, respectively. The lifetime is close to the parallel characterization of Shao's work [24]. Though the input signal given a pulse injection, the output signal was reshaped to exponentials due to the capacitance and resistor inside of PERC.

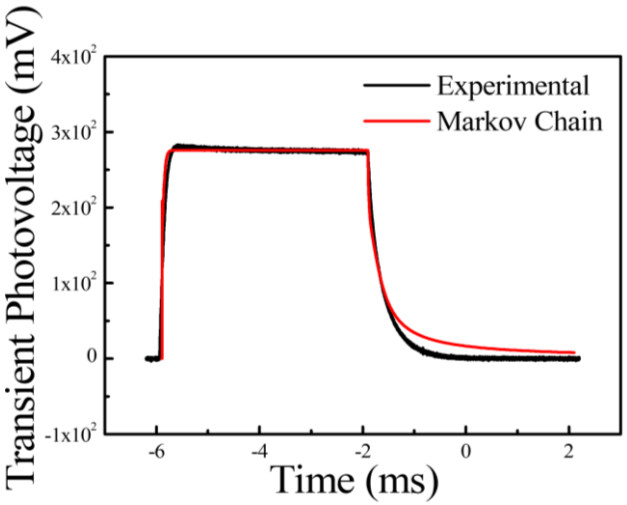

Fig. 5. The transient photovoltage and Markov mathematical approach (color online)

The simulation results based on the Markov approach was basically consistent with the experimental result. The raising edge was very close to the experimental model because the parameters and probability were well predicted in transient process. However, the falling edge was followed the same tendency at the beginning but separated at the end of the curve decay. An important reason is that the Markov Chain was assumed under thermal equilibrium (T = 300 k) condition, however, the experimental result exhibited a faster decay due to the thermal effect of laser. With the phonon injection, more deep level traps were excited, known as Light and elevated Temperature Induced Degradation (LeTID), to accelerate the charge decay.

5. Conclusion

In this article, we have simulated the excitation and decay in PERCs based on the Markov Approach, it can be seen that the simulation followed the same tendency with the experimental model with charging and discharging effect with lifetime of 175 μs and 782 μs, respectively. However, the model cannot perfectly explain the thermal induced traps such as LeTID effect. In the following research, the dynamic thermal condition can be introduced to describe probability and expectation of carrier behaviors. This model can also be expanded into other field such as photo detectors and LEDs to further explain the carrier behaviors inside of semiconductors.

Acknowledgement

We acknowledge the funding from Zhejiang Provincial Innovation Team (2019R01012).

References

[1] M. A. Green, E. D. Dunlop, J. Hohl-Ebinger, M. Yoshita, N. Kopidakis, A. W. Y. Ho-Baillie, Progress in Photovoltaics **28**(7), 629 (2020).
[2] A. H. Muhammad, Solar Energy **197**, 163 (2020).
[3] W. X. W. Tress, Advanced Materials **31**(44), 1902851 (2019).
[4] Y. Tong, Z. Xiao, X. Du, C. Zuo, Y. Li, M. Lv, Y. Yuan, C. Yi, F. Hao, Y. Hua, T. Lei, Q. Lin, K. Sun, D.i Zhao, C. Duan, X. Shao, W. Li, H. L. Yip, Z. Xiao, B. Zhang, Q. Bian, Y. Cheng, S. Liu, M. Cheng, Z. Jin, S. Yang, L. Ding, Science China-Chemistry **63**(6), 758 (2020).
[5] F. Gao, Y. Zhao, X. Zhang, J. You, Advanced Energy Materials **10**(13), 1902650 (2020).
[6] E. Gervais, S. Shammugam, L. Friedrich, T. Schlegl, Renewable and Sustainable Energy Reviews **137**, 110589 (2021).
[7] P. Wang, R. Sridharan, X. Ng, J. Ho, R. Stangl, Solar Energy Materials and Solar Cells **220**, 110834 (2021).
[8] X. Li, H. Dong, S. Guo, L. Zhao, Applied Sciences-BASEL **10**(14), 4857 (2020).
[9] C. Sun, M. M. Mroz, J. Cabanillas-Gozalez, L. Lüer, D. Hermida-Merino, C. Zhao, M. Takeuchi, K. Sugiyasuc, J. Cabanillas-González, Journal of Material Chemistry C **6**, 6591 (2019).

[10] A. Isakova, S. Karuthedath, T. Arnold, J. R. Howse, P. D. Topham, D. T. W. Toolan, F. Laquai, L. Luer, Nanoscale **10**, 10934 (2018).
[11] S. Karuthedath, T. Sauermann, H. J. Egelhaaf, R. Wannemacher, C. J. Brabecd, L. Luer, Journal of Materials Chemistry A **3**, 3399 (2015).
[12] R. S. Torrientes, A. Gavrik, A. Isakova, A. Abudulimu, J. Calbo, J. Aragó, J. Santos, E. Ortí, N. Martín, V. Dyakonov, L. Luer, Journal of Materials Chemistry C **7**, 6641 (2019).
[13] M. S. Alvar, P. W. M. Blom, G. J. A. H. Wetzelaer, Nature Communications **11**(1), 4023 (2020).
[14] K. Wang, D. Yang, C. Wu, M. Sanghadasab, S. Priya, Progress in Materials Science **106**, 100580 (2019).
[15] J. Carolus, J. A. Tsanakas, A. V. D. Heide, E. Voroshazi, W. D. Ceuninck, M. Daenen, Solar Energy Materials and Solar Cells **200**, 109950 (2019).
[16] Y. Zhang, L. Wang, D. Chen, M. Kim, B. Hallam, Journal of Physics D-Applied Physics **54**(21), 214003 (2021).
[17] F. Haase, B. Min, C. Hollemann, J. Krügener, R. Brendel, R. Peibst, Progress in Photovoltaics **29**(5), 516 (2021).
[18] S. Maus, F. Maischner, S. Riepe, J. Greulich, E. Lohmüller, F. Schindler, P. Saint-Cast, P. Krenckel, A. Hess, S. Lohmüller, A. Wolf, R. Preu, Solar RRL **5**(4), 2000752 (2021).
[19] K. Y. Choo, S. V. Muniandy, K. L. Woon, M. T. Gan, D. S. Ong, Organic Electronics **41**, 157 (2017).
[20] L. Villegas-Lelovsky, G. Gonzalez de la Cruz, Y. G. Gurevich, Thin Solid Films **433**(1-2), 371 (2003).
[21] X. Du, L. Luer, T. Heumuller, J. Wagner, C. Berger, T. Osterrieder, J. Wortmann, S. Langner, U. Vongsaysy, M. Bertrand, N. Li, T. Stubhan, J. Hauch, C. J. Brabec, Joule **5**(2), 495 (2021).
[22] A. J. Baddeley, M. N. M. Vanlieshout, J. Moller, Advances in Applied Probability **28**(2), 346 (1996).
[23] S. Succi, P. Vergari, VLSI Design **6**, 137 (1998).
[24] J. Shao, X. Xi, G. Liu S. Li, R. Peng, G. Chen, Y. Jiang, Bulletin of Materials Science **43**(1), 262 (2020).

*Corresponding author: yifeng.he@beyondsunpv.com